JOURNAL OF SOLID STATE CHEMISTRY 57, 82–96 (1985)

# Indirect Metal–Metal Interactions in Solids: Relation with Polarization and Charge Density Waves*

C. HAAS

*Laboratory of Inorganic Chemistry, Materials Science Centre, University of Groningen, Nijenborgh 16, 9747 AG Groningen, The Netherlands*

Received June 5, 1984; in revised form August 2, 1984

Metal–metal bonding may arise from a direct overlap of metal orbitals. However, an indirect interaction between metal atoms is also possible. It is shown that the presence of a highly polarizable medium around positively charged metal atoms leads to an effective metal–metal interaction. In insulating ionic compounds the anions serve as the polarizable medium. This leads to a clustering of metal atoms in layers or chains in compounds with highly polarizable anions. In compounds with metallic conduction the conduction electrons provide the polarizable medium. The instability of conduction electrons in linear-chain and layered compounds leads to charge density waves and the associated clustering of metal atoms. © 1985 Academic Press, Inc.

## 1. Introduction

In many inorganic solids the metal atoms form clusters of different shapes and sizes, such as infinite linear or zigzag chains (one-dimensional clusters, 1D), layers with a high concentration of metal atoms alternating with layers without metal atoms (two-dimensional clustering, 2D), or isolated clusters (0D) such as pairs, triangles, tetrahedra, or octahedra of metal atoms. In recent years a very large number of compounds with such metal clusters have been prepared and their interesting properties have been investigated (*1–6*).

In the most naive pictures of chemical bonding one does not expect a close approach of metal atoms in compounds which contain metal as well as nonmetal atoms. For example, in a simple ionic model one expects the bonding to be mainly due to the Coulomb attraction between the positively charged metal atoms and the negatively charged nonmetal atoms. Also, in a covalent description of the chemical bonding one expects strong (polar) bonds, in particular between metal and nonmetal atoms. As a consequence one expects a close approach between metal and nonmetal atoms, and a spatial arrangement of the atoms in the molecule or the crystal such that the distance between the equally charged metal atoms is as large as possible.

Nevertheless, as mentioned already, in many compounds short metal–metal distances are observed, indicating some kind of metal–metal interaction. In this paper we will discuss the origin of this interaction. We will show that, in addition to direct

* Presented at the Symposium on Metal–Metal Bonding in Solid State Clusters and Extended Arrays, held during the American Chemical Society meeting, St. Louis, Missouri, April 9–10, 1984.

0022-4596/85 $3.00

covalent bonding between metal atoms, also indirect interactions are possible which lead to an effective metal–metal attraction. In general the indirect interaction between the metal atoms occurs via a strongly polarizable medium consisting of highly polarizable anions or of conduction electrons for metals.

## 2. Direct Metal–Metal Bonding

(*a*) *Heitler–London vs molecular orbital approach.* In this paragraph we review briefly the Heitler–London (HL) and the molecular orbital (MO) model for the covalent bonding between two metal atoms. These two models are by no means equivalent. We will show from experiments on a particular binuclear transition metal complex that in that compound the wavefunction is described much better by the HL model (*7, 8*).

We consider the simple case of two atoms A and B at a fairly large distance from each other, each with one electron in a simple nondegenerate orbital; we disregard the overlap integral between the orbitals. The Hamiltonian of the system (which is similar to that of the $H_2$ molecule) is

$$H = \sum_{\sigma} \varepsilon_{\sigma}(c^{+}_{A\sigma}c_{A\sigma} + c^{+}_{B\sigma}c_{B\sigma}) + \sum_{\sigma} t(c^{+}_{A\sigma}c_{B\sigma} + c^{+}_{B\sigma}c_{A\sigma}) + U(n_{A\uparrow}n_{A\downarrow} + n_{B\uparrow}n_{B\downarrow}) \quad (1)$$

in which $c^{+}_{A\sigma}$ and $c_{A\sigma}$ are creation and annihilation operators for electrons with spin $\sigma$ in the orbital $\varphi_A$ on atom A. The product $n_{A\sigma} = c^{+}_{A\sigma}c_{A\sigma}$ corresponds to the number of electrons with spin $\sigma$ in orbital $\varphi_A$, and can have the values $n_{A\sigma} = 0, 1$. The first term in (1) represents the orbital energy of the electron on one atom. The second term is the transfer contribution; the transfer integral is $t = \langle\varphi_A|h|\varphi_B\rangle$, where $h$ is the one-electron Hamiltonian operator. The last term of (1) represents the electron correlation energy, and is an expression for the electrostatic repulsion between the two electrons. For this interaction we use the Hubbard form: the electron–electron repulsion is taken into account only to the extent that the electrons reside on the same atom. This so-called "on site" Coulomb integral $U$ is

$$U = \langle\varphi_A(1)\varphi_A(2)|\nu(r_{12})|\varphi_A(1)\varphi_A(2)\rangle. \quad (2)$$

In a simple system with only two electrons $\nu_{12} = e^2/r_{12}$, in a more complex system the Coulomb repulsion is partly screened by other electrons. We disregard two-center exchange integrals like $\langle\varphi_A(1)\varphi_B(2)|\nu(r_{12})|\varphi_B(1)\varphi_A(2)\rangle$ (the so-called potential exchange); this is justified for large distances between the two atoms.

First we discuss the electronic states for the case without transfer ($t = 0$). We then have a covalent singlet state

$$\phi_1 = [\varphi_A(1)\varphi_B(2) + \varphi_B(1)\varphi_A(2)]\chi_s/\sqrt{2} \quad (3)$$

and a covalent triplet state

$$\phi_2 = [\varphi_A(1)\varphi_B(2) - \varphi_B(1)\varphi_A(2)]\chi_T/\sqrt{2}. \quad (4)$$

These two HL states have one electron on each atom and have (for $t = 0$) the same energy $E_1 = E_2 = 2\varepsilon_0$.

There are also two ionic singlet states with energy $E_3 = E_4 = 2\varepsilon_0 + U$ and wavefunctions

$$\phi_3 = \varphi_A(1)\varphi_A(2)\chi_s \quad \phi_4 = \varphi_B(1)\varphi_B(2)\chi_s. \quad (5)$$

In these expressions $\chi_s$ and $\chi_T$ are singlet and triplet spin functions $\chi_s = (1/\sqrt{2})$ $[\alpha(1)\beta(2) - \beta(1)\alpha(2)]$ and $\chi_T = \alpha(1)\alpha(2)$; $\beta(1)\beta(2)$; $(1/\sqrt{2})[\alpha(1)\beta(2) + \beta(1)\alpha(2)]$, where $\alpha(1)$ represents electron 1 with spin up ($m_s = +1/2$), etc.

The introduction of transfer results in a mixing of covalent and ionic states. The new singlet ground state is

$$\phi_s = \phi_1 \cos\theta - (1/\sqrt{2})(\sin\theta)(\phi_3 + \phi_4) \quad (6)$$

with $\tan 2\theta = 4t/U$, and as energy

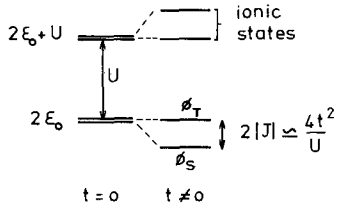


FIG. 1. Energy levels in a $H_2$-like system.

$$E_s = 2\varepsilon_0 + \tfrac{1}{2}U - \tfrac{1}{2}\sqrt{U^2 + 16t^2}. \quad (7)$$

The triplet states $\phi_T = \phi_2$ remain unchanged by the transfer, and have the energy $2\varepsilon_0$. Thus we find that the singlet state has a lower energy than the triplet state. The energy difference $\Delta E = \frac{1}{2}U - \frac{1}{2}\sqrt{U^2 + 16t^2}$ can be regarded as the energy of the covalent bond between the two atoms. We can also regard this energy as an effective exchange energy between the two electrons: the transfer $t$ produces an effective antiferromagnetic coupling between the spins of the two electrons. For $2|t| \ll U$ we obtain the well-known result for kinetic exchange $2J \simeq 4t^2/U$ (Anderson) (Fig. 1).

The ionicity of the singlet ground state can be defined as $\kappa = \sin^2\theta$; for small $t$ we find $\kappa \simeq (2t/U)^2$. Thus for small transfer (large distance between the atoms) the ionicity is small, and the Heitler–London description is appropriate. The electrons are nearly localized, and the contribution of ionic states in the wavefunction of the ground state is small. For large transfer the electrons are delocalized, and the contribution of ionic states is large. In the limit $2|t| \gg U$ (i.e., for large $t$ and small $U$) the ionicity is $\kappa = 0.5$ and we have the molecular-orbital-type description with the two ground-state electrons in a bonding orbital $\varphi_g = (1/\sqrt{2})(\varphi_A + \varphi_B)$.

An important question is whether a particular system is best described by a localized (HL) or a delocalized (MO) picture. The MO model is more frequently used, presumably because it is easier to extend the MO method to larger systems with more electrons and atoms. However, especially for relatively weak bonds one expects the HL model to be more realistic. This was shown to be the case for the binuclear complex $(C_{10}H_8)$ $(C_5H_5)_2$ $Ti_2Cl_2$ (*7, 8*) (Fig. 2). This molecule has two identical Ti atoms, each with one $3d$ electron. Therefore the interaction between the two Ti atoms can be described with the $H_2$-like model described above.

The magnetic susceptibility $\chi$ of the complex (Fig. 2) increases with temperature ($T$); this is due to the increased population of the triplet states $\phi_T$ which have a magnetic moment (spin $S = 1$). The temperature dependence of $\chi$ is then given by

$$\chi = \frac{Ng^2\mu_B^2 S(S+1)}{kT[3 + \exp - (2J/kT)]} \quad (8)$$

because the energy of the triplet state is $-2J \simeq 4t^2/U$, and its magnetic moment is $g\mu_B\sqrt{S(S+1)}$. The observed curve of $\chi$ versus $T$ could be fitted quite well with this expression with $-2J = 0.06$ eV (Fig. 2).

The photoelectron spectrum of the complex shows in the valence region two peaks with ionization energies of 5.82 and 6.17 eV (Fig. 3). As the two Ti($3d$) electrons in the ground state are identical, we must attribute the two peaks to two different final

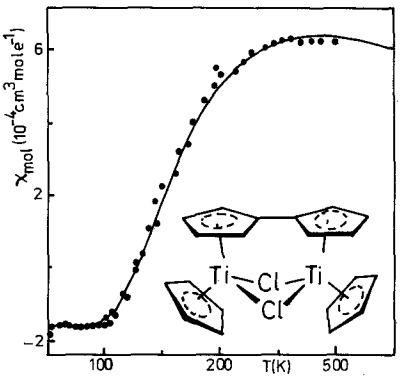


FIG. 2. Molar susceptibility of $(C_{10}H_8)(C_5H_5)_2Ti_2Cl_2$ versus temperature. The full curve shows the theoretical fit to the experimental points (dots).

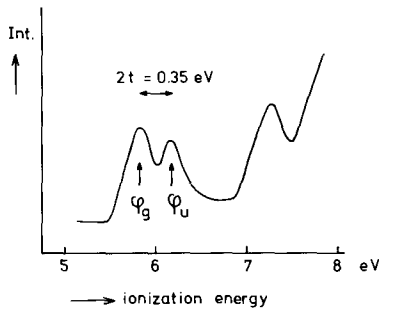


FIG. 3. Photoelectron spectrum of $(C_{10}H_8)(C_5H_5)_2Ti_2Cl_2$ with HeI excitation. The two peaks at 5.82 and 6.17 eV are due to ionization of a Ti(3*d*) electron, leading to two different final states with the remaining Ti(3*d*) electron in orbitals $\varphi_g$ and $\varphi_u$, respectively.

states: the one at 5.82 eV with an electron in the bonding orbital $\varphi_g = (1/\sqrt{2})(\varphi_A + \varphi_B)$, the peak at 6.17 eV corresponding to an electron in the antibonding orbital $\varphi_u = (1/\sqrt{2})(\varphi_A - \varphi_B)$. The energy difference between the two peaks is $2t = 0.35$ eV.

The intensity ratio of the two peaks in the photoelectron spectrum is given by $I_u/I_g = |(1 + \tan\theta)/(1 - \tan\theta)|^2$, and is a direct measure of the contribution of ionic states to the ground-state wavefunction. For a HL ground state ($\tan\theta = 0$) we have $I_u/I_g = 1$; for a MO ground state ($\tan\theta = -1$), $I_u/I_g = 0$ and only a single main peak is observed. The large intensity $I_u$ of the satellite peak (Fig. 3) shows directly that the ground state is mainly of the HL type.

From these data we calculate $U = 2$ eV and $t = 0.175$ eV and an ionicity $\kappa = 0.03$. Thus, the ionicity in the ground state is quite small; the contribution of ionic states is only 3%. Therefore, a molecular orbital description of metal–metal bonding in this complex is not allowed; the Ti(3*d*) electrons are highly localized and should be described with a HL model.

In discussions on bonding in metal clusters and complexes one frequently uses MO theory without thoroughly investigating first whether HL or MO theory is more appropriate. This may lead to serious errors, as shown by the example discussed above.

(*b*) *Distortion of a linear chain of metal atoms.* It is well known that metal–metal bonding in a crystal can lead to a distortion of the crystal structure (*9–11*). We first discuss the simple case of a linear chain of equally spaced metal atoms, with spacing *a*. We assume that this chain of metal atoms is imbedded in a crystal (of nonmetal atoms), which determines the total length of the chain of $N + 1$ atoms to be $Na$ (Fig. 4). The interaction between two metal atoms is given by a function $V(r)$, which represents the covalent chemical bonding between the atoms and, at short distances, the repulsion (Fig. 5). In addition there will be an elastic energy $\frac{1}{2}fu^2$, required to displace an atom over a distance *u* from the center of the site it occupies in the undistorted structure.

The energy of the undistorted structure with *N* equally spaced atoms is $E_0 = NV(a)$. In a dimerized chain (Fig. 5) there are alternating short strong chemical bonds (length $a - u$) and long weak bonds (length $a + u$). The energy of the dimerized chain is

$$E_d = \tfrac{1}{2}NV(a - u) + \tfrac{1}{2}NV(a + u) + \tfrac{1}{2}Nfu^2. \quad (9)$$

The undistorted chain becomes unstable if $E_d < E_0$, which is the case if $(\delta^2V/\delta r^2)_{r=a} < -f$. Then a spontaneous dimerization (pair

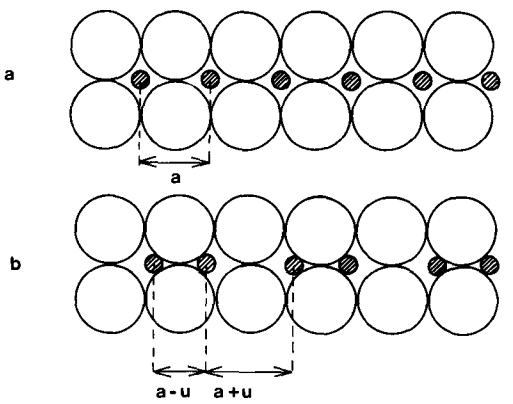


FIG. 4. Metal–metal bonding in a linear chain of metal atoms imbedded in a matrix of nonmetal atoms. (a) Undistorted, (b) dimerized.

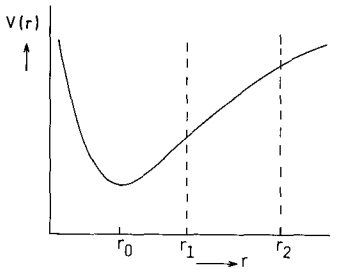


FIG. 5. Interaction $V(r)$ between two metal atoms. The dimerized chain is stable in the region $r_1 < a < r_2$.

formation) will occur. The reason for the dimerization is essentially that the sum of the energy of a short bond $(a - u)$ and a long bond $(a + u)$ is lower than the energy of two bonds of intermediate length.

Many cases of dimerization in linear chains have been observed. We mention the case of $VO_2$: below 340 K the $V^{4+}(3d^1)$ ions form covalently bonded pairs along the $c$-axis (*12–14*). Above 340 K the thermal motion destroys the long-range order of pairs and a tetragonal phase with higher symmetry is found, in which the average metal–metal distances along the chain are equal. Another example is that of $NbS_3$ (and many other Nb compounds), where pairs of $Nb^{4+}(4d^1)$ ions with very short Nb–Nb distances are found (*15, 16*). Many donor–acceptor complexes, such as those of TCNQ molecules, have a crystal structure with linear stacks of the flat TCNQ molecules. In several of these (metallic) compounds these stacks at low temperature undergo a phase transition in which a pairing of the TCNQ molecules takes place (*17*). In these cases the chemical bonding between the TCNQ molecules replaces the metal–metal bonding in linear chains of metal atoms.

In all these cases the dimerization occurs in metallic systems, and the distortion to a dimerized state is usually described as a Peierls distortion (*18*), related to the instability of a 1D electron gas of conduction electrons. Although this may very well be the origin of the observed dimerization in most or all cases, the considerations given above show that dimerization is a very general phenomenon and that metallic conductivity is not a necessary condition for the effect to occur.

With the simple model of chemical bonds it is also possible to understand the occurrence of incommensurate distortions in linear chains (*19*). Consider again a linear chain of atoms and take into account not only interactions between nearest, but also between next-nearest neighbors. The total energy is given by

$$E = \frac{1}{2}\sum_n [f_1(u_n - u_{n+1})^2 + f_2(u_n - u_{n+2})^2], \quad (10)$$

where $u_n$ is the (small) displacement of the $n$th atom, and $f_1 = (\delta^2 V/\delta r^2)_{r=a}$, $f_2 = (\delta^2 V/\delta r^2)_{r=2a}$. The energy of a sinusoidal distortion, characterized by a wave vector $q$ and periodicity $\lambda = 2\pi a/q$, with atomic displacement $u_n = u \cos qna$, is

$$E = \tfrac{1}{2}Nu^2[f_1(1 - \cos qa) + f_2(1 - \cos 2qa)]. \quad (11)$$

The lowest energy is obtained for a modulation with a wave vector $q_0$ given by $\cos q_0 a = -f_1/4f_2$; this modulation is stable for $f_1 > 0, f_2 < 0, f_1 < 4|f_2|$. A model of this type can be used to describe incommensurate distortions in insulating compounds, such as $NaNO_2$ (*20*), $Na_2CO_3$ (*21*), $K_2SeO_4$ (*22*), and $Rb_2ZnBr_4$ (*23*).

Similar considerations have been used earlier to explain incommensurate magnetic structures, resulting from competing near neighbour and next nearest neighbour interactions (*50*).

(*c*) *Distortion in a hexagonal layer of metal atoms*. Next, we discuss distortions of a simple two-dimensional hexagonal lattice of metal atoms, as present in many transition metal chalcogenides with a layered structure. We assume that the overall dimensions of the lattice are determined by

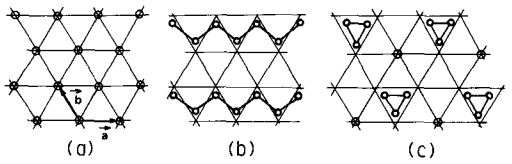


FIG. 6. Distortions of a 2D hexagonal lattice. (a) Undistorted; (b) MnP-type distortion, with $q_1 = (0, 1/2)$ and zigzag chains of atoms; (c) Low-temperature NbS-type distortion with triangles, a superposition of three zigzag chains.

(repulsive) interactions between the larger nonmetal atoms in the crystal. We will show that a simple, isotropic attractive interaction between the metal atoms imbedded in such a structure of nonmetal atoms, can lead to quite complicated lattice distortions and clustering of metal atoms (*9, 10*).

In the model we consider an elastic interaction $\frac{1}{2}fu^2$, which binds each metal atom to a particular site, and a metal–metal interaction $V(r)$ of the type shown in Fig. 5. An arbitrary distortion is characterized by displacements $\mathbf{u}_n = \mathbf{R}_n - \mathbf{n}$ of the metal atom from its site $\mathbf{n} = n_1\mathbf{a} + n_2\mathbf{b}$ in the undistorted structure ($\mathbf{a}$ and $\mathbf{b}$ are the lattice vectors of the hexagonal lattice). The total energy is

$$E = \frac{1}{2}\sum_n fu_n^2 + \frac{1}{2}\sum_n \sum_s V(|\mathbf{R}_{n+s} - \mathbf{R}_n|). \quad (12)$$

The second summation is taken over all nearest-neighbors lattice sites of $\mathbf{n}$, i.e., $\mathbf{s} = \pm\mathbf{a}, \pm\mathbf{b}, \pm(\mathbf{a} + \mathbf{b})$.

We now calculate the energy $E_q = A_q|\mathbf{u}_q|^2$ for a small distortion of the lattice with wave vector $\mathbf{q}$ and atomic displacements $\mathbf{u}_n = \mathbf{u}_q e^{i\mathbf{q}\cdot\mathbf{n}}$. The distortion with the lowest energy is obtained by minimizing the energy; we obtain as stable solutions the undistorted state ($u_n = 0$), and three equivalent distortions $\mathbf{q}_1 = (0, 1/2)$ with $\psi = 90°$; $\mathbf{q}_2 = (1/2, 0)$ with $\psi = -30°$, and $\mathbf{q}_3 = (1/2, 1/2)$ with $\psi = +30°$ ($\psi$ is the angle between the atomic displacements $\mathbf{u}_n$ and the $\mathbf{a}$ axis). Each of these solutions corresponds to a zigzag chain of metal atoms (Fig. 6). The relative stability depends on the interaction function $V(r)$ and the average distance $a$; for a sufficiently large value of $a$ the distorted structure is stable.

The energy of a linear combination of the equivalent zigzag chain solutions is the same as far as quadratic terms $A_q|\mathbf{u}_q|^2$ are concerned, but not for higher-order terms. For a solution with $u_{q1} = u\gamma_1$, $u_{q2} = u\gamma_2$, $u_{q3} = u\gamma_3$, the third-order terms vanish, and the fourth-order terms in the energy are

$$E_4 = Nu^4[D_1 + D_2(\gamma_1^2\gamma_2^2 + \gamma_2^2\gamma_3^2 + \gamma_3^2\gamma_1^2)]. \quad (13)$$

The coefficients $D_1$ and $D_2$ depend on the derivatives of $V(r)$. By minimizing the energy with respect to $\gamma_1$, $\gamma_2$, and $\gamma_3$, one finds that the zigzag chain solution ($\gamma_1 = 1$, $\gamma_2 = 0$, $\gamma_3 = 0$) is stable for $D_2 > 0$; for $D_2 < 0$ a linear combination with $\gamma_1 = \gamma_2 = \gamma_3 = 1/\sqrt{3}$ is more stable (*24*). This linear combination consists of isolated atoms and triangular clusters of metal atoms with short bonds (Fig. 6). Indeed, this type of distortion has been observed as the structure of Nb atoms in the low-temperature (l.t.) form of NbS (*25, 26*). If we take for the metal–metal interaction a function $V(r) = (1/12)A(r/r_0)^{-12} - (1/6)A(r/r_0)^{-6}$, we find that the l.t. NbS-type structure is stable with respect to the MnP-type structure with zigzag chains in the region $a < 1.273\, r_0$ (Fig. 7).

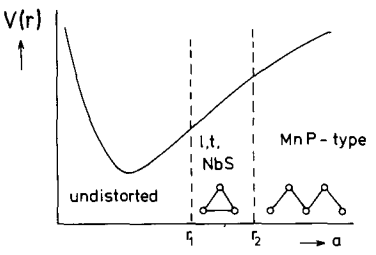


FIG. 7. Stability of distortions of a hexagonal layer.

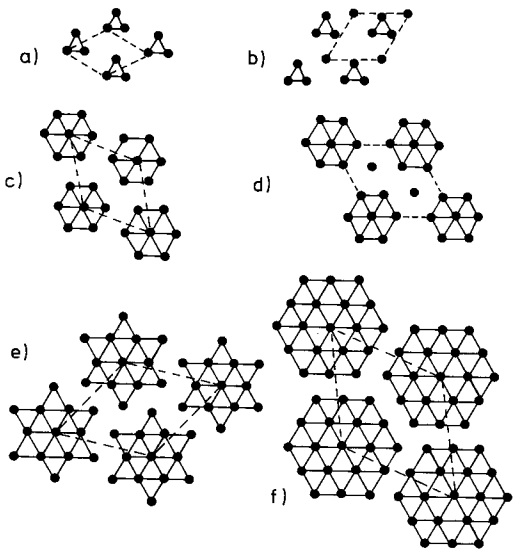


FIG. 8. Trigonal distortions of hexagonal layers, with clusters of metal atoms: (a) $q$ = (2/3, 1/3) – FeS (*27*); (b) $q$ = (1/2, 0) – low-temperature NbS (*25*); (c) $q$ = (2/7, 1/7) – $VSe_2$ (*28*); (d) $q$ = (1/3, 0) – $VSe_2$ (*28*), 2H – $TaSe_2$, 2H – $NbSe_2$ (*1*); (e) $q$ = (4/13, 1/13) – 1T – $TaS_2$, 1T – $TaSe_2$ (*29, 30*); (f) $q$ = (2/19, 1/19) – $NbTe_2$, $TaTe_2$ (*31*).

These considerations show that the distortions with zigzag chains (MnP type) and triangular clusters (l.t. NbS type) represent in a sense the natural distortions of a simple hexagonal layer. For a linear chain the metal–metal attraction between nearest neighbors leads to dimers; this is not so for a hexagonal lattice. This explains in a very general way why indeed distortions with a pairing of atoms have not been observed for hexagonal layers. For the formation of the fairly complicated distortion patterns as the MnP and l.t. NbS type it is not necessary to invoke directed bonds or the like; an isotropic attraction between the metal atoms is sufficient. The zigzag-chain-type distortion of a hexagonal layer has been observed in many compounds, such as VS, MnP, MnAs, $MoTe_2$, $NbTe_2$, and $TaTe_2$ (*25, 26*).

The MnP and l.t. NbS-type distortions were obtained by considering only interactions between nearest neighbors. If one takes into account also interactions between more distant metal atoms in the hexagonal layer also one finds that more complicated distortions can be stable. Among these are incommensurable distortions, i.e., distortions with a periodicity not compatible with the hexagonal lattice. The calculated distortions exhibit clusters of metal atoms, with clusters of 3, 7, 13, or 19 atoms (Fig. 8). In most cases these complicated distortion patterns are attributed to the charge density wave mechanism, to be discussed in Section 4. We have shown in this section that these distortions can also be obtained with a simple model of metal–metal bonding, but that the more complicated distortion patterns (large clusters, incommensurate structures) are found only if more long-range interactions are taken into account. We will show later that the interaction with conduction electrons in metals provides this type of long-range interaction between the metal atoms.

## 3. Metal Clusters in Ionic Crystals

We discuss in this section the clustering of metal atoms based on a simple ionic model, in which the molecule or crystal consists of polarizable ions.

Consider first, as an introductory example, the water molecule. In an ionic model each proton has a charge $+e$, the oxygen ion a charge $-2e$. In spite of the electrostatic repulsion between the two protons, the molecule is not linear: it is as if there existed an effective attraction between the hydrogen atoms. This attraction is due to the polarization of oxygen. If the H–O–H angle is $2\theta$ (Fig. 9), the electric field at the oxygen ion is $F = (2e/R^2)\cos\theta$, and the polarization energy is $-\frac{1}{2}\alpha F^2 = -(2e^2\alpha/R^4)\cos^2\theta$ ($\alpha$ is the polarizability of oxygen). Thus, the total energy as a function of the H–H distance $r = 2R\sin\theta$ can be written as

$$V(r) = A + e^2/r + Br^2. \qquad (14)$$

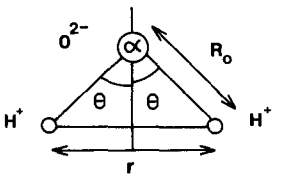


FIG. 9. Ionic model of water molecule.

We have kept the O–H distance fixed (due to the strong covalent bond) at $R_0$, and $A = -2e^2\alpha/R_0^4$, $B = e^2\alpha/2R_0^6$. The minimum energy is obtained for a distance $r = R_0^2\alpha^{-1/3}$. Of course, this simple model does not give an accurate description of the structure and the chemical bond of the water molecule, but it demonstrates at least qualitatively that polarization can lead to an effective attraction between positive ions. The polarization energy tends to concentrate charge as much as possible, in order to make the polarization energy as large as possible.

We now apply these simple concepts to ionic crystals and, in particular, to crystals with a layered structure (such as $CdI_2$) (*11, 32–34*). The layered structure of $CdI_2$ can be considered as a 2D type of metal clustering. In the hexagonal close packing of the anions the cations occupy the octahedral holes. However, the cations occupy the octahedral sites in alternating layers, leaving other layers empty (van der Waals gap, see Fig. 10). Thus, the cations cluster in hexagonal layers. The reason for this apparent clustering has been known for a very long time to be the polarization of the anions.

We discuss ionic crystals $MX_2$, with positive ions of charge $+2Ze$, and negative ions with charge $-Ze$. The total energy is given by

$$E = -\frac{NAZ^2e^2}{R} + NBR^{-n} - \frac{CNZ^2e^2\alpha}{R^4}\left(1 + \frac{D\alpha}{R^3}\right)^{-1}. \quad (15)$$

The first term is the Madelung energy: $A$ is the Madelung constant, $N$ is the number of cations in the crystal, and $R$ is the characteristic (shortest) cation–anion distance. The second term is the Born repulsion between the ions, with a parameter $B$; $n$ is a number between 6 and 12. The last term is the polarization energy. In general there will be an electric field at the anion due to the charges of all ions in the crystal; this field produces a polarization of the anions with polarizability $\alpha$ (for simplicity we disregard the polarizability of the cation). The factor $[1 + (D\alpha/R^3)]^{-1}$ represents a correction due to the contribution of the induced dipoles to the total electric field. $A$, $C$, and $D$ are constants for the lattice sums of the fields of charges and dipoles, and depend on the crystal structure. In equilibrium the total energy is a minimum; from the condition $\delta E/\delta R = 0$ it is possible to eliminate $B$. The result is

$$E = -\frac{NAZ^2e^2}{R}\left(1 - \frac{1}{n}\right) - \frac{NZ^2e^2}{R} \times C\beta(1 + D\beta)^{-1}\left[1 - \frac{4}{n} + \frac{3D\beta}{n(1 + D\beta)}\right] \quad (16)$$

with $\beta = \alpha/R^3$.

A simple structure in which many $MX_2$ compounds crystallize is the fluorite structure $C1$ ($CaF_2$ structure). This is the structure with the highest Madelung constant $A(C1) = 5.0388$; therefore, this structure has the lowest energy of all $MX_2$ structures if only the Madelung energy is considered. In this structure the electric field at the anion vanishes, so that the polarization energy is zero ($C = 0$). In the layered structures $CdI_2$ ($C6$) and $CdCl_2$ ($C19$) the anions have a strongly asymmetric coordination of three cations, which induces an electric di-

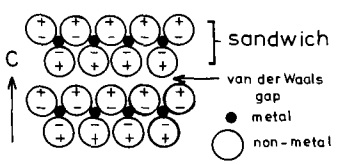


FIG. 10. $CdI_2$-type layer structure: clustering of metal atoms in alternating layers.

TABLE I

CRYSTAL STRUCTURES $MX_2$, LISTED IN THE ORDER OF DECREASING RADIUS OF THE CATION (*35*)

| | $R_M$ (Å) | F | Cl | Br | I |
|---|---|---|---|---|---|
| $Ba^{2+}$ | 1.36 | *C*1 | *C*1, *C*23 | *C*23 | *C*23 |
| $Pb^{2+}$ | 1.18 | *C*1 | *C*23 | *C*23 | *C*6* |
| $Sr^{2+}$ | 1.16 | *C*1 | *C*1 | *C*53 | — |
| $Ca^{2+}$ | 1.00 | *C*1 | *C*35 | *C*35 | *C*6* |
| $Cd^{2+}$ | 0.95 | *C*1 | *C*19* | *C*19* | *C*6* |
| $Mn^{2+}$ | 0.82 | *C*4 | *C*19* | *C*6* | *C*6* |
| $V^{2+}$ | 0.79 | — | *C*6* | *C*6* | *C*6* |
| $Fe^{2+}$ | 0.77 | *C*4 | *C*19* | *C*19* | *C*6* |
| $Zn^{2+}$ | 0.75 | *C*4 | *C*19* | *C*19* | *C*6* |
| $Co^{2+}$ | 0.74 | *C*4 | *C*19* | *C*19* | *C*6* |
| $Mg^{2+}$ | 0.72 | *C*4 | *C*19* | *C*6* | *C*6* |
| $Ni^{2+}$ | 0.70 | *C*4 | *C*19* | *C*19* | *C*19* |
| | | O | S | Se | Te |
| $Th^{4+}$ | 1.00 | *C*1 | *C*23 | *C*23 | — |
| $Zr^{4+}$ | 0.72 | *C*1 | *C*6* | *C*6* | *C*6* |
| $Hf^{4+}$ | 0.71 | *C*1 | *C*6* | *C*6* | *C*6* |
| $Sn^{4+}$ | 0.69 | *C*5 | *C*6* | *C*6* | — |
| $Pt^{4+}$ | 0.63 | *C*6* | *C*6* | *C*6* | *C*6* |
| $Ti^{4+}$ | 0.61 | *C*4 | *C*6* | *C*6* | *C*6* |

*Note.* Layered structures are indicated by an asterisk.

pole at the anions. For the ideal $CdI_2$ structure $C = 7.29$ and $D = 3.613$, and if $\alpha$ is large the polarization energy can be appreciable. On the other hand, the Madelung constant of $CdI_2$ is smaller, $A(C6) = 4.3819$. We find that the $CdI_2$ structure is stable with respect to the $CaF_2$ structure for $\beta > 0.2069$ (for $n = 9$). Thus, the $CdI_2$ structure is stable for large $\alpha$ and small $R$, as expected. This is indeed what is observed. In Table I we have listed the metal dihalides and dichalcogenides in order of decreasing $R$, and we find that the layer structures $C6$ and $C19$ occur for compounds with small $R$. The stability region of the layer structures is larger for anions with large $\alpha$. Layer structures are not found for the fluorides and the oxides, due to the small values of $\alpha$ for $F^-$ and $O^{2-}$. Thus, with this simple model of polarizable ions, we can explain the stability of these layered structures.

We now consider briefly a number of cases with short metal distances (clustering) and investigate whether the polarizability could be responsible for, or at least contribute, to the clustering.

The polarization of the anions is caused by an asymmetric coordination of anions by cations. Therefore it is possible to gain further polarization energy in a hexagonal layer by distorting the hexagonal symmetry, for example, as in the zigzag chains (MnP-type structure) and triangles of cations (l.t. NbS-type structure) (Fig. 6). A simple calculation (*9*) shows that these distortions indeed lead to a further increase of the polarization energy, and that they are expected to be stable if $(\alpha/R^3)$ is larger than a critical value. This suggests that large distortions of hexagonal layers will be observed in compounds with small cations and highly polarizable anions. Indeed, especially the ditellurides, with the highly polarizable $Te^{2-}$ ion, exhibit these distortions: $MoTe_2$, $WTe_2$, $NbTe_2$, $TaTe_2$ (*25, 26*), and $VTe_2$ (*36*). We remark that one would not expect this result if direct metal–metal bonding were the origin of the distortion: in that case the distortions would be weakest in the ditellurides, because of the larger metal–metal distances.

The polarization also explains some structural aspects of the transition metal chalcogenides $MX_3$ and $MX_4$. The crystals $NbX_3$ and $TaX_3$ ($X$ = S, Se) (*25, 26, 37*) contain linear chains of metal atoms; each metal atom is surrounded by a trigonal prism of two $X^{2-}$ and two $X_2^{2-}$ anions (Fig. 11). In $TaTe_4$ and $NbTe_4$ (*25, 26, 38*) there are also linear chains of metal atoms, and each metal atom is coordinated by eight Te in the form of a tetragonal antiprism. In all these crystals the metal–metal distances in the chain are much shorter than between metal atoms in different chains. The coordination of the highly polarizable anions is strongly asymmetric, providing a large polarization energy. The average metal–metal

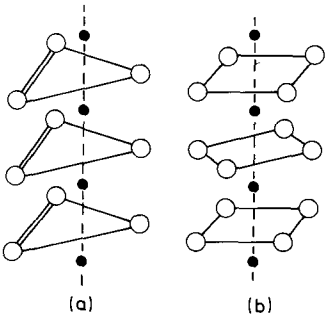


FIG. 11. Structure of $MX_3$(a) and $MTe_4$(b), with $M$ = Nb, Ta; $X$ = S, Se. The average metal–metal distances along the chain are about 3.40 Å (distances in the pure metals Nb and Ta are about 2.90 Å).

distances in the chain are fairly short as in the $MX_2$ compounds, but by no means as short as in the pure metals. Several of these linear-chain compounds show further (often incommensurate) distortions, leading to short and long metal–metal distances along the chain (*15, 16, 36*).

In the polarizable ion model the crystal structure is a compromise between Madelung energy favoring large cation–cation distances, and the polarization energy favoring an asymmetric coordination of polarizable anions. This principle can be used to understand the crystal structures of many inorganic solids (*32, 39*). The metal trihalides $FeCl_3$, $CrCl_3$, $BiI_3$, etc. crystallize in layered structures derived from the $CdI_2$ or $CdCl_2$ structures. In the partly occupied layers the metal atoms form an ordered array in which the repulsive energy between the cations is a minimum. In the intercalated materials $A_xMX_2$ ($A$ = Na, Cu, Ag; $X$ = S, Se) (*40*) the structure is usually such that the cations with the highest charge ($M$) occupy alternate layers, as in $CdI_2$. The remaining cations of lower charge, $A$, occupy sites in the van der Waals gap. In this manner the anion coordination by cation charges is as asymmetric as is compatible with the composition of the crystal. Examples of this rule are $Cr_3S_4$ (fully occupied $Cr^{3+}$ layers alternate with half-occupied $Cr^{2+}$ layers), $Cr_2S_3$ (fully occupied $Cr^{3+}$ layers alternate with one-third-occupied $Cr^{3+}$ layers), $Na_xTiS_2$, $Ag_xCrS_2$, etc. (fully occupied Ti, Cr layers, $Na^+$ and $Ag^+$ in the van der Waals gap).

Thus, the simple polarizable ion model can explain a considerable amount of structural data of inorganic compounds. The model also explains the observed strong anisotropy of the polar lattice vibrations of layered crystals, and the fact, related to this, that the softening of the perpendicular modes serves as a precursor to the distortion of hexagonal layers (*34*). However, we remark that anion polarization is certainly not the only mechanism which drives the lattice distortions in layered materials. An example is $TiSe_2$, which at low temperature has a distorted structure with a unit cell $2a \times 2a \times 2c$ (*41*), the same unit cell as l.t. NbS, but with atomic displacements quite different from those of the l.t. NbS structure. A calculation shows that the atomic displacements in $TiSe_2$ are of a type which is not favored by anion polarization. Calculations in which the distortions in $TiSe_2$ are attributed to a band Jahn–Teller effect (metal $d$–nonmetal $p$ hybridization) are in excellent agreement with experimental data (*42*). This mechanism is related with the charge density wave mechanism and with the contribution of charge transfer transitions (metal–nonmetal hybridization) to the polarizability.

## 4. Charge Density Waves

Several metallic crystals undergo phase transitions which are attributed to instabilities of the conduction electrons (*1*). The possibility of such an electron-gas instability and the resulting lattice distortion was recognized for the first time by Peierls (*18*), who showed that a 1D crystal with a half-filled band is unstable with respect to a distortion which leads to a doubling of the unit cell.

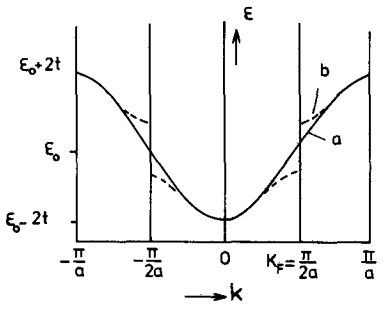


FIG. 12. Energy band for a linear chain of atoms. (a) Undistorted (drawn line), (b) dimerized (dotted line).

We begin with the discussion of a Peierls distortion (a charge density wave, CDW) of a linear chain of atoms at positions $na$, each with one electron in a nondegenerate orbital $\varphi$. In the tight-binding approximation (which corresponds to the MO model, with large transfer $t$, and $U = 0$), the wavefunction $\psi$ is a molecular orbital (or Bloch wave) extending over the entire chain of atoms, characterized by a wave vector $k$.

$$\psi_k(r) = \frac{1}{\sqrt{N}} \sum_n e^{ikna} \varphi(r - na), \quad (17)$$

where $\varphi(r - na)$ is the atomic orbital of atom $n$ at position $na$. The transfer integral between nearest-neighbor sites is $t = \langle \varphi(r)|H|\varphi(r - a)\rangle$, and we disregard the overlap integrals $\langle \varphi(r)|\varphi(r - a)\rangle = 0$. The eigenvalues for the energy $\varepsilon_k = \varepsilon_0 - 2t \cos ka$ form an energy band (Fig. 12). If there is one electron per atom, this band is half-filled, up to the Fermi energy $\varepsilon_F = \varepsilon_0$ and the Fermi wave vector $k_F = \pi/2a$; the crystal will exhibit metallic conductivity.

Next we study the effect of a displacement of the atoms on the electronic energy levels. A periodic distortion with atomic displacements $u_n = u_0 \exp iqna$, characterized by a wave vector $q$, will lead to an extra potential energy $\delta V(r) = \delta V_q \exp iqr$ which perturbs the electrons. This perturbation has matrix elements $\delta V_q$ between wave functions $\psi_{k+q}$ and $\psi_k$, and this leads to the formation of energy gaps in the band structure at $k = \pm\frac{1}{2}q$. For a distortion with $q_0 = 2k_F$ the energy gaps occur just at the Fermi energy $\varepsilon_F$. Because in that case the states occupied by electrons are lowered in energy, the distortion $q_0 = 2k_F$ will produce a lowering of the total energy of the crystal (Fig. 12). Due to excitations of electrons and vibrations of the atoms, the energy gaps will gradually disappear with increasing temperature and vanish at a certain critical temperature $T_0$. Thus, at $T_0$, the crystal with the distorted structure transforms to an undistorted state. Due to the gaps in the energy band, the crystal in the distorted state is semiconducting. Therefore, the phase transition at $T_0$ for a linear chain corresponds to a metal-to-semiconductor transition (*43*).

For a 1D crystal with one electron per atom $k_F = \pi/2a$, and therefore the wave vector of the distortion is $q = 2k_F = \pi/a$. This corresponds to a displacement of the atoms by $u_n = (-1)^n u_0$, i.e., to a dimerized chain (Fig. 12).

The formation of a CDW can be considered also from a different point of view (*44*). A CDW can be defined as a static periodic change of electron density coupled with a periodic lattice distortion. We discuss again the 1D model with positive ions at equal distances $a$, imbedded now in a uniform electron charge density $\rho_0$ (Fig. 13). The CDW corresponds to a periodic change of the conduction electron density

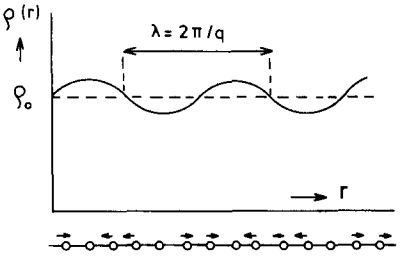


FIG. 13. Charge density wave and periodic lattice distortion of a linear chain of atoms.

$\Delta\rho(r) = A \cos qr$. This partial localization of electronic charge in space will cost interelectronic repulsion energy and electron kinetic energy. However, the positive ions will move in response to the new charge distribution. This effect will lower the total energy; it corresponds to a clustering of metal atoms in the crystal at places with a higher negative electron charge density. If this electron–phonon interaction is sufficiently strong it is possible that the ground state of the crystal is a distorted state (CDW).

The distortion of the lattice produces a change of the effective potential for the electron $\delta V(r) = \delta V_q \exp iqr$ and this induces a change of the electron density proportional to $\delta V(r)$:

$$\Delta\rho(r) = \chi(q)\delta V_q e^{iqr}. \qquad (18)$$

The proportionality factor $\chi(q)$ is the response function of the electron gas. For large values of $\chi(q)$ a small perturbation with wave vector $q$ will already produce an appreciable change of the electron density and, as a consequence, a large distortion. For $\chi(q_0) \rightarrow \infty$ the crystal is unstable against distortion $q_0$, and will distort spontaneously. For a free-electron gas the response function is

$$\chi_0(q) = \sum_k \frac{f_k(1 - f_{k+q})}{\varepsilon_{k+q} - \varepsilon_k}, \qquad (19)$$

where $\varepsilon_k$ is the energy of an electron state $k$, and $f_k$ is the Fermi distribution function $f_k = [1 + \exp(\varepsilon_k - \varepsilon_F)/kT]^{-1}$. For an electron gas with interactions we can write

$$\chi(q) = \frac{\chi_0(q)}{1 - W(q)\chi_0(q)}, \qquad (20)$$

where $W(q)$ takes account of electron–electron and electron–phonon interactions.

The response function $\chi_0(q)$ depends strongly on the dimensionality of the electron gas (Fig. 14). For a 1D electron gas $\chi_0$ diverges at $q_0 = 2k_F$; therefore a 1D metal will distort spontaneously with a periodicity characterized by a wave vector $q_0 = 2k_F$ (Peierls distortion; CDW).

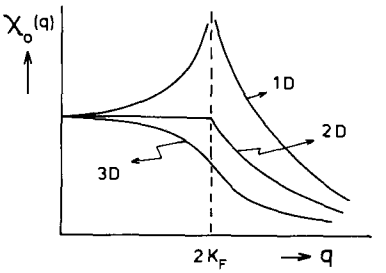


FIG. 14. Response function $\chi_0(q)$ for a free-electron gas in one, two, and three dimensions (1D, 2D, 3D).

For a free-electron gas in two or three dimensions the singularity of $\chi_0(q)$ at $q = 2k_F$ is much weaker. However, in a real crystal it is possible that certain parts of the Fermi surface have 1D or 2D character. Generally, a large value of $\chi(\mathbf{q}_0)$ is obtained if the Fermi surface contains large areas connected by $\mathbf{q}_0$ with parallel tangent planes. This is the so-called "nesting" which is responsible for the strong CDWs in layered compounds (*1*).

Many examples of CDW distortions in layered crystals have been detected with electron or X-ray diffraction. A particularly well-studied case is that of 1T-$TaS_2$, a compound for which not only the symmetry and the periodicity of the distortion were determined, but also the actual atomic displacements (*29, 30*). The commensurate distortion in the layers in 1T-$TaS_2$, stable below 200 K, corresponds to a superposition of CDWs characterized by the wave vectors $\mathbf{q}_1 = (4/13, 1/13)$, $\mathbf{q}_2 = (-1/13, 3/13)$, and $\mathbf{q}_3 = (-3/13, -4/13)$. In this structure the Ta atoms form clusters of 13 atoms (see Fig. 8). In other layered compounds complicated distortion patterns have also been observed, but in most cases the actual positions of the atoms in the distorted structure have not been determined. Some examples with the postulated metal clusters compatible with the translational symmetry are shown in Fig. 8.

A detailed discussion of the theory of commensurate and incommensurate CDW distortions in terms of the Landau theory of phase transitions has been given by W. L. McMillan (*51–53*).

## 5. Direct and Indirect Metal–Metal Interactions

In the preceding sections we described several mechanisms which lead to short metal–metal distances and to metal clustering. First there is the direct interaction between the metal atoms, due to the formation of a chemical bond. However, we have shown that short metal–metal distances can also be obtained by interaction with a polarizable medium, consisting of polarizable anions (Section 3) or conduction electrons (Section 4). In this section we show that the interaction via a polarizable medium can be expressed in terms of an effective indirect interaction between the metal atoms (*45, 46*).

We first show that the (Peierls) instability of an electron gas in combination with an electron–phonon interaction leads to an effective metal–metal interaction which is of long range and oscillating. For the vibronic part of the Hamiltonian we write

$$H = \frac{1}{2}\sum_q P_q^2 + \frac{1}{2}\sum_q \omega_0^2(q)u_q^2 + \sum_q g(q)u_q e^{iqr}. \quad (21)$$

The first term is the kinetic energy, the second term, the potential energy of the lattice vibrations with amplitude $u_q$, wave vector $q$, and frequency (in the absence of coupling with the electron) $\omega_0(q)$. If the displacement of atom $n$ is $u_n$, then $u_q$ is defined as $u_q = \Sigma_n u_n e^{iqn}$. The last term in (21) is the electron–phonon interaction, with a coupling constant $g(q)$. We now calculate with perturbation theory the change of the electron energy due to electron–phonon coupling; the result for a free-electron gas is given by

$$\Delta E_{\text{el.}} = \sum_q \sum_k \frac{f_k(1 - f_{k+q})}{\varepsilon_k - \varepsilon_{k+q}} g^2(q)u_q^2 = -\sum_q g^2(q)\chi_0(q)u_q^2. \quad (22)$$

Therefore, the Hamiltonian for the lattice vibrations in the presence of the electron gas is

$$H_{\text{vibr.}} = \frac{1}{2}\sum_q P_q^2 + \frac{1}{2}\sum_q \{\omega_0^2(q) - 2g^2(q)\chi_0(q)\}u_q^2, \quad (23)$$

i.e., the interaction with the electron gas induces a change of the vibration frequencies given by

$$\omega^2(q) = \omega_0^2(q) - 2g^2(q)\chi_0(q). \quad (24)$$

This lowering of the phonon frequencies (phonon softening) is the so-called Kohn anomaly (*43, 47*). The strong decrease of $\omega(q)$ at $q = 2k_F$, i.e., where $\chi_0(q)$ has a maximum, has been observed quite clearly in 1D metals such as $K_2Pt(CN)_4Br_{0.3}(H_2O)_3$ (this compound contains linear chains of Pt atoms, with metallic conductivity along the chains) (*48*).

We now transform $E_{\text{el.}}$ into an interaction between the metal atoms by substituting $u_q = \Sigma_n u_n e^{iqn}$:

$$\Delta E_{\text{el.}} = \frac{1}{2}\sum_n \sum_{n'} f_{nn'} u_n u_{n'} \quad (25)$$

with $f_{nn'} = -2\sum_q g^2(q)\chi_0(q)e^{iq(n-n')}$

For small displacements $u_n$ this is equivalent to an effective interaction $V(R)$ between metal atoms at a distance $R = n - n' + u_n - u_{n'}$ if $(\delta^2 V/\delta R^2)_{R=n-n'} = -f_{nn'}$. Therefore, the electron–phonon interaction energy $\Delta E_{\text{el.}}$ can be represented by an effective metal–metal interaction

$$V(R) = -\sum_q \frac{2g^2(q)\chi_0(q)}{q^2} e^{iqR}. \quad (26)$$

In a 1D metal $\chi_0(q)$ is very large at $q_0 = \pm 2k_F$, and we obtain a large contribution to

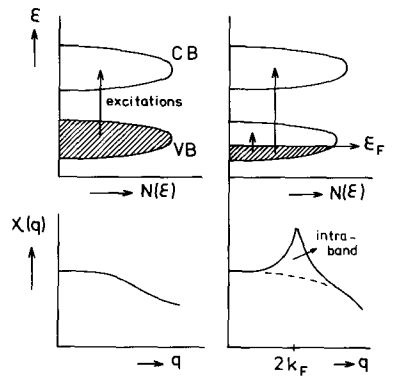


FIG. 15. Contributions of electronic excitations to the response function $\chi(q)$ of electrons for insulators (left-hand side: only interband transitions) and metals (right-hand side: inter- and intraband transitions).

$V(R)$ from the electrons near the Fermi energy. This contribution is of the form

$$\sim \frac{2g^2(2k_F)\chi_0(2k_F)}{4k_F^2} \cos 2k_F R. \qquad (27)$$

It is long range and oscillating, and it is, of course, precisely this contribution to the metal–metal interaction which induces the periodic lattice distortion of the CDW. We remark that the long-range oscillating interaction due to electrons near $\varepsilon_F$ is well known for the interaction between charged impurities in metals (*49*).

The derivation given for the effective metal–metal interaction is also valid for insulators and semiconductors. In that case, however, the electron susceptibility does not diverge because there is a finite gap between occupied and unoccupied states.

As we have seen, there is close relation between the polarization mechanism and the CDW mechanism for effective metal–metal interaction. In an insulator the interaction is due to virtual excitations from the valence band to the conduction band over a finite gap; these excitations are excitations on the atoms (atomic or ionic polarizability) or charge transfer excitations. A large number of electron states (all states in the valence band) contribute, and the contribution to the metal–metal interaction is large if the polarizability is large.

If the polarizability of the crystal is given by a sum of ionic polarizabilities, the corresponding $\chi(q)$ has only a weak $q$ dependence and the interaction is relatively short range. The metal–metal interactions caused by virtual charge transfer excitations are equivalent with the so-called band Jahn–Teller effect used to explain the distortion in $TiSe_2$ (*38*).

In a metal the mechanism due to virtual interband transitions will also operate, but there is an additional contribution from intraband transitions of electrons near the Fermi energy. This contribution gives rise to a pronounced peak in $\chi(q)$ near $q = 2k_F$, and it produces a long-range oscillating metal–metal interaction responsible for the complicated CDW distortions.

## References


1. J. A. WILSON, F. J. DISALVO, AND S. MAHAJAN, *Adv. Phys.* **24,** 117 (1975).
2. K. YVON, *Curr. Top. Mater. Sci.* **3,** 53 (1979).
3. B. F. G. JOHNSON AND J. LEWIS, *Adv. Inorg. Chem. Radiochem.* **24,** 225 (1981).
4. J. S. MILLER AND A. J. EPSTEIN, *Progr. Inorg. Chem.* **20,** 1 (1976).
5. A. SIMON, *Angew. Chem.* **93,** 23 (1981).
6. H. G. VON SCHNERING, *Angew. Chem.* **93,** 44 (1981).
7. J. C. GREEN, R. RANKIN, E. A. SEDDON, J. H. TEUBEN, A. H. JONKMAN-BEUKER, AND D. K. G. DE BOER, *Chem. Phys. Lett.* **82,** 92 (1981).
8. D. K. G. DE BOER, thesis, Groningen (1983).
9. C. HAAS, *Solid State Commun.* **26,** 709 (1978).
10. C. HAAS, *Curr. Top. Mater. Sci.* **3,** 1 (1979).
11. C. HAAS, *in* "Physics of Layered Compounds" (L. Pietronero and E. Tosatti, Eds.), p. 158, Springer-Verlag, New York/Berlin (1981).
12. J. B. GOODENOUGH, *Progr. Solid State Chem.* **5,** 145 (1971).
13. D. ADLER AND H. BROOKS, *Phys. Rev.* **155,** 826 (1967).
14. A. ZYLBERSZTEJN AND N. F. MOTT, *Phys. Rev. B* **11,** 4383 (1975).
15. J. RIJNSDORP AND F. JELLINEK, *J. Solid State Chem.* **25,** 325 (1978).

16. J. RIJNSDORP, thesis, Groningen (1978).
17. H. J. KELLER, Ed., "Chemistry and Physics of One-Dimensional Metals," Plenum, New York (1977).
18. R. E. PEIERLS, "Quantum Theory of Solids," Oxford Univ. Press (Clarendon), London/ New York (1955).
19. R. PYNN, *Nature (London)* **281,** 433 (1979).
20. Y. YAMEDA, I. SHIBUYA, AND S. HOSHINO, *J. Phys. Soc. Jpn.* **18,** 1594 (1963).
21. C. M. FORTUIN, *Physica A* **86,** 224 (1977).
22. M. TIZUMI, J. D. AXE, AND G. SHIRANE, *Phys. Rev. B* **15,** 4392 (1977).
23. C. J. DE PATER AND C. VAN DIJK, *Phys. Rev. B* **18,** 1281 (1978).
24. H. F. FRANZEN, C. HAAS, AND F. JELLINEK, *Phys. Rev. B* **10,** 1248 (1974).
25. F. HULLIGER, *in* "Structural Chemistry of Layer-Type Phases" (F. Lévy, Ed.), p. 247, Reidel, Dordrecht (1976).
26. F. HULLIGER, *Struct. Bonding* **4,** 83 (1968).
27. J. M COEY, H. ROUX-BUISSON, AND R. BRUSETTI, *J. Phys. (Paris) C* **4,** 1 (1976).
28. J. VAN LANDUYT, G. A. WIEGERS, AND S. AMELINCKX, *Phys. Status Solidi A* **46,** 479 (1978).
29. R. BROUWER AND F. JELLINEK, *Physica B* **99,** 51 (1980).
30. R. BROUWER, thesis, Groningen, 1978.
31. J. VAN LANDUYT, G. VAN TENDELO, AND S. AMELINCKX, *Phys. Status Solidi A* **26,** 585 (1974).
32. A. E. VAN ARKEL, "Moleculen en Kristallen," van Stockum & Zoon, Den Haag (1961).
33. Y. M. DE HAAN, *in* "Molecular Dynamics and the Structure of Solids" (R. S. Carter and J. J. Rush, Eds.), p. 233, Nat. Bur. Standards, Washington, D.C. (1969).
34. C. HAAS, *Physica B* **105,** 305 (1981).
35. R. D. SHANNON AND C. T. PREWITT, *Acta Crystallogr. Sect. B* **25,** 925 (1969).
36. K. D. BRONSEMA, G. W. BUS, AND G. A. WIEGERS, *J. Solid State Chem.* **53,** 415 (1984).
37. J. L. HODEAU, M. MAREZIO, C. ROUCAU, R. AYROLES, A. MEERSCHAUT, J. ROUXEL, AND P. MONCEAU, *J. Phys. C* **11,** 4117 (1978).
38. K. D. BRONSEMA AND S. VAN SMAALEN, to be published.
39. F. JELLINK, *in* "Inorganic Sulphur Chemistry" (G. Nickless, Ed.), p. 670, Elsevier, Amsterdam (1968).
40. G. V. SUBBA RAO AND M. W. SHAFER, *in* "Intercalated Layered Materials" (F. A. Lévy, Ed.), p. 99, Reidel, Dordrecht (1979).
41. F. J. DISALVO, D. E. MONCTON, AND J. V. WASZCZAK, *Phys. Rev. B* **14,** 4321 (1976).
42. Y. YOSHIDA AND K. MOTIZUKI, *J. Phys. Soc. Jpn.* **49,** 898 (1980).
43. M. J. RICE AND S. STRÄSSLER, *Solid State Commun.* **13,** 125 (1973).
44. F. J. DISALVO, *in* "Electron–Phonon Interactions and Phase Transitions" (T. Riste, Ed.), Plenum, New York (1978). NATO Adv. Study Inst. Ser. B: Physics.
45. L. J. SHAM, *Phys. Rev.* **188,** 1431 (1969).
46. R. M. PICK, M. H. COHEN, AND R. M. MARTIN, *Phys. Rev. B* **1,** 910 (1970).
47. W. KOHN, *Phys. Rev. Lett.* **2,** 393 (1959).
48. B. RENKER, H. RIETSCHEL, L. PINTSCHOVIUS, W. GLÄSER, P. BRÜESCH, D. KUSE, AND M. J. RICE, *Phys. Rev. Lett.* **30,** 1144 (1972).
49. J. FRIEDEL, *in* "Theory of Magnetism in Transition Metals," Italian Physical Society: Proc. Int. School of Physics "Enrico Fermi" (W. Marshall, Ed.), p. 283, Academic Press, New York (1967).
50. J. C. SMART, Effective Field Theories of Magnetism, W. B. Saunders, Philadelphia, 1966.
51. W. L. MCMILLAN, *Phys. Rev. B* **12,** 1187 (1976).
52. W. L. MCMILLAN, *Phys. Rev. B* **14,** 1996 (1976).
53. W. L. MCMILLAN, *Phys. Rev. B* **16,** 643 (1977).